scientific reports

Check for updates

OPEN

Route to high-T_c superconductivity of BC_7 via strong bonding of boron–carbon compound at high pressure

Prutthipong Tsuppayakorn-aek[1,2], Xiaoyong Yang[3], Prayoonsak Pluengphon[4], Wei Luo[3], Rajeev Ahuja[3,5] & Thiti Bovornratanaraks[1,2]✉

We have analyzed the compositions of boron–carbon system, in which the BC_7 compound is identified as structural stability at high pressure. The first-principles calculation is used to identify the phase diagram, electronic structure, and superconductivity of BC_7. Our results have demonstrated that the BC_7 is thermodynamically stable in the diamond-like $P\bar{4}m2$ structure at a pressure above 244 GPa, and under temperature also. Feature of chemical bonds between B and C atoms is presented using the electron localization function. The strong chemical bonds in diamond-like $P\bar{4}m2$ structure are covalent bonds, and it exhibits the s–p hybridization under the pressure compression. The Fermi surface shape displays the large sheet, indicating that the diamond-like $P\bar{4}m2$ phase can achieve a high superconducting transition temperature (T_c). The outstanding property of BC_7 at 250 GPa has manifested very high-T_c of superconductivity as 164 K, indicating that the carbon-rich system can induce the high-T_c value as well.

Carbon-rich material at high pressure and high temperature is interesting due to its outstanding properties to be super-hardness and superconductors. With regards to the study of boron carbides, a $BC_{1.6}$ phase has been observed using synchrotron-based X-ray diffraction, Raman spectroscopy, and energy-dispersive scanning electron microscopy[1]. The results have revealed that the *g*-$BC_{1.6}$ structure transforms to the diamond-like $BC_{1.6}$ at a temperature of 2230 K and a pressure of 45 GPa. They demonstrated that BC_x can transform to hexagonal-$BC_{1.6}$ or orthorhombic-$BC_{1.6}$, depending upon the pressure and temperature conditions. However, the heating is not enough to make transformation to the cubic phase. Successfully, a cubic BC_3 structure has been synthesized at a pressure of 39 GPa and a temperature of 2200 K using a laser-heated diamond anvil cell,which the system is condensed by the sp^3 hybridization[2].

In the progress for finding the word record of the highest superconducting transition temperature (T_c)[3], the novel compositions in the interesting compounds have been reported at high pressure conditions. The hydrogen-rich materials of H_3S[4] and LaH_{10}[5] were proposed to be superconductor at gigapascal pressures (203 K and 250 K), which the high-T_c temperature superconductivity depended on the conventional electron–phonon coupling and the shape of density of states around the Fermi level[6]. The high pressures above 100 GPa on these materials were required for structural stabilities of the rich hydrides. It was introduced that another material to find the better superconductors can be applied by the same concepts and methods[3]. Therefore, the high-pressure effect is one of the crucial tool for the formation of the atom-rich system, and the discovery of high-T_c superconductivity. In another way to enhance the high-T_c superconductivity, alkali-doped C_{60} system has been presented as a superconducting material among carbon related compounds. The T_c in the alkali-doped C_{60} was reported as 33 K, which moderated by the coupling of electrons to high-frequency molecular vibrational modes[7].

[1]Extreme Conditions Physics Research Laboratory (ECPRL) and Physics of Energy Materials Research Unit, Department of Physics, Faculty of Science, Chulalongkorn University, Bangkok 10330, Thailand. [2]Thailand Centre of Excellence in Physics, Ministry of Higher Education, Science, Research and Innovation, 328 Si Ayutthaya Road, Bangkok 10400, Thailand. [3]Condensed Matter Theory Group, Department of Physics and Materials Science, Uppsala University, Box 530, 751 21 Uppsala, Sweden. [4]Division of Physical Science, Faculty of Science and Technology, Huachiew Chalermprakiet University, Samutprakarn 10540, Thailand. [5]Applied Materials Physics, Department of Materials and Engineering, Royal Institute of Technology (KTH), 100 44 Stockholm, Sweden. ✉email: thiti.b@chula.ac.th

In the carbon-rich systems, the experimental study has been reported the synthesis of cubic BC_5 (c-BC_5), which is the diamond-like structure. The c-BC_5 was synthesized at a pressure of 24 GPa and a temperature of 2200 K using both laser-heated diamond anvil cell and large-volume multi anvil apparatus. The synthesized c-BC_5 showed that it is too high Vickers hardness (H_v) up to 71 GPa[8]. Moreover, the BC_5 phase is suggested as a candidate structure at high pressure through ab initio random search calculation. The $I\bar{4}m2$ structure was introduced as the most stable structure at high pressure. By the density functional theory (DFT) study, it was reported that the predicted $I\bar{4}m2$ structure is metallic, and the estimated T_c of the superconducting phase is as 47 K[9]. In another class of boron carbides, the BC_7 was predicted as a candidate structure under high pressure using particle swarm optimization (PSO) methodology[10]. The BC_7 compound was the stable composition in the diamond-like $I\bar{4}m2$ structure, and also exhibited to be a super-hard material with the H_v as 75.2 GPa. In addition, the effect of temperature has been presented as an influence for structural phase transformation of boron carbides such as $BC_{1.6}$ and BC_3, while the phase diagram boundaries of the boron carbides are still incomplete.

Keeping all these carbon-rich in mind, another class of carbides, the BC_7 phase predicted as a candidate structure under high pressure using particle swarm optimization (PSO) methodology[10]. Predictions of BC_7 revealed that the most stable structure is the diamond-like $P\bar{4}m2$ structure, and also exhibits superhard materials with the Vickers hardnesses of 75.2 GPa. They suggested that the diamond-like $P\bar{4}m2$ structure can be thermodynamically stable at ambient to high pressure (100 GPa). It is known that boron carbides are the most popular materials for experimental and theoretical investigations, in fact, the effect of temperature has an influence for structural phase transformation of boron carbides, such as $BC_{1.6}$ and BC_3.

Recently, the phase diagram of B-C system has been investigated from ambient to high pressure and under temperature effect[11]. The report showed that the effect of temperature is an important role for thermodynamically stable structure as well. In this work, the class of BC_7 phase is a point of interest for finding phase diagram with quasi-harmonics approximation (QHA), which can calculate thermodynamics properties also. Therefore, the main attention is to investigate the phase diagram of BC_7 and the structural searching analysis. The perspective of theoretical inspection displays a thermodynamically stable phase via the QHA calculation. The presence of route to high-Tc superconductivity via decomposition of binary diamond-like BC_7 compound is described through the Allen–Dynes equation.

Computational details

The structure searching of the BC_7 was performed by the Universal Structure Predictor: Evolutionary Xtallography (USPEX) code[12] combined with the Vienna ab initio simulation package (VASP) code[13]. In all subsequent generations, the random symmetric algorithm, which consisted of 40% heredity, 20% random symmetric, 20% softmutation, and 20% transmutation operators in the pressure range from 0 to 300 GPa with structures containing up to 4 formula units. All of the DFT calculations in this work used the generalized gradient approximation of the Perdew–Burke–Ernzerhof (GGA–PBE) functional[14] for the exchange-correlation functional. We employed the projector augmented wave (PAW) method[15], as implemented in the VASP code. The PAW potentials were applied with a plane wave basis set up to a cutoff energy of 700 eV and a 10 × 10 ×4 k-point mesh for the diamond-like $P\bar{4}m2$ structure, which was generated by the Monkhorst–Pack (MP) method[16]. The pseudocore radii of C and B are 1.1 Bohr and 1.1 Bohr, respectively, which are small enough that the overlap of spheres will not occur under applied pressure. All of the structural parameters were fully relaxed by using the Methfessel–Paxton smearing method[13] and the conjugate gradient scheme. All considered structures were relaxed at each pressure until the Hellman–Feynman forces became less than 10^{-3} eV/Å. The phonon calculation was calculated using the ab initio lattice dynamics with the linear response method as implemented in the VASP code together with the PHONOPY package[17], which is an important role for investigation of the phase stability in metallic system[18–20]. The cutoff energy and k-point set for the phonon linear response calculation were used as 700 eV and 10 × 10×4 for a 3 × 3×2 supercell (144 atoms) in the diamond-like $P\bar{4}m2$ structure at 250 GPa. We calculated elastic constants for the diamond-like $P\bar{4}m2$ structure, as implemented in the CAmbridge Serial Total Energy Package (CASTEP) code[21]. In the superconducting phase, we calculated the electron–phonon coupling (EPC) within the density functional perturbation theory[22]. via Quantum Espresso (QE) package[23]. The PAW potentials were employed in QE. The plane-wave energy cutoff of 60 Ry was used. The Brillouin zone (BZ) integrations in the electronic and phonon calculations were performed using the MP meshes. The EPC matrix elements were computed in the first BZ on 4 × 4×2 q-meshes using individual EPC matrices obtained with a 24 × 24×16 k-points mesh. The Allen–Dynes equation[24] was used with the effective Coulomb pseudopotential parameter, $\mu^* = 0.10$ (0.13) as follows;

$$T_c = \frac{\omega_{log}}{1.2} \exp\left[-\frac{1.04(1+\lambda)}{\lambda - \mu^*(1+0.62\lambda)}\right], \quad (1)$$

where ω_{log} is the logarithmic average of the spectral function, and λ is the total electron–phonon coupling strength. We found that λ value are less than 1.5 in most of our work, thus this form of Allen–Dynes equation is quite sufficient.

Results and discussion

To investigate the structural formation of binary diamond-like BC_7 compound, we present the thermodynamically stable structures of B and B-doped diamond in Fig. 1a,b. Structural phase transitions of B under high pressure are analyzed. The α-B structure transforms to the γ-B structure at 26 GPa, and then it transforms to the α -Ga-type structure at 98 GPa. The calculation displayed that the α-Ga-type structure is the most stable structure (Fig. 1a). It is induced that the direct transformation from graphite to diamond structure at 15 GPa[25]. The diamond structure is the most stable structure and its stable structure can be used for identifying BC_7 structure. A

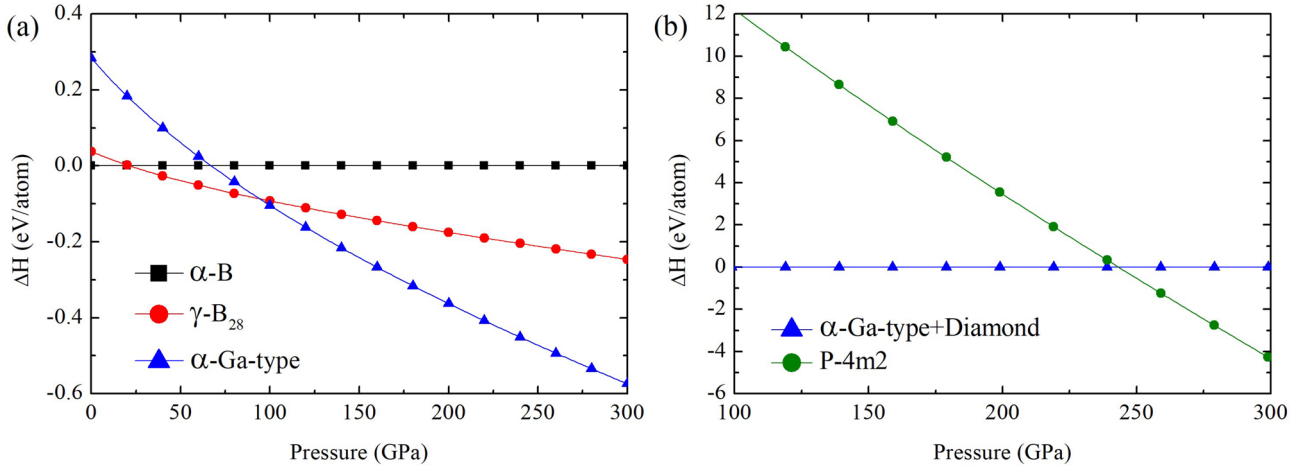

Figure 1. (**a**) The enthalpies-pressure relation of boron and (**b**) the enthalpies-pressure relation of BC_7.

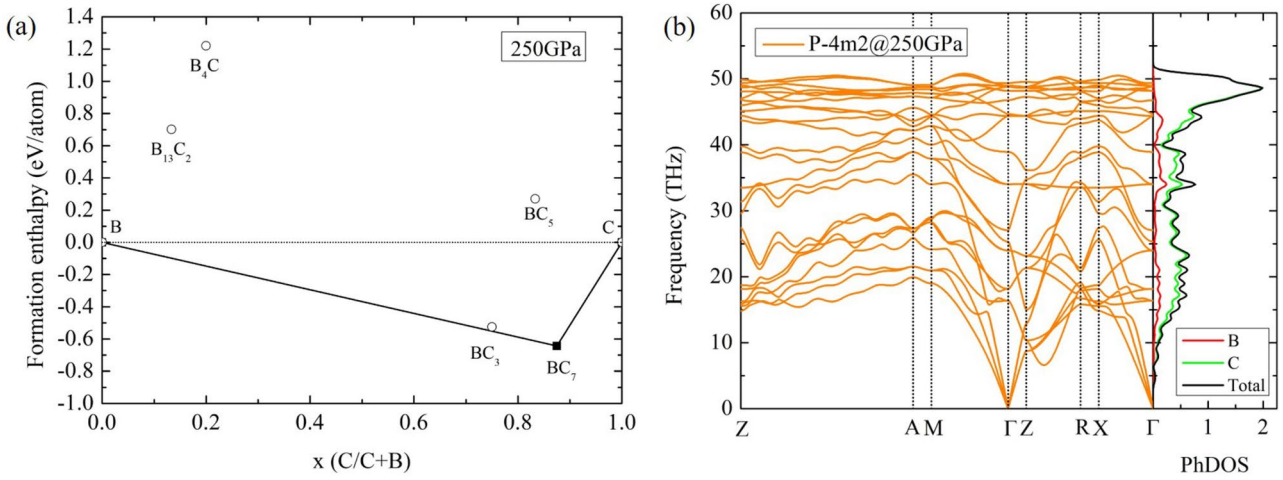

Figure 2. (**a**) Formation enthalpy of BC_7 presented in convex hull at 250 GPa and (**b**) the phonon dispersion and the phonon density of states of the diamond-like $P\bar{4}m2$ at 250 GPa.

predicted structure can be obtained from USPEX code. It is found that the decomposition of α-Ga-type+diamond transforms to the diamond-like $P\bar{4}m2$. This is shown that the diamond-like $P\bar{4}m2$ structure can be formed above 244 GPa, as seen in Fig. 1b. The diamond-like $P\bar{4}m2$ structure is thermodynamically stable at pressure above 244 GPa, as shown in Fig. 1b. To investigate a formation of the diamond-like $P\bar{4}m2$ structure in BC7, it is focused on decomposition of B+C above 100 GPa. Convex hull of the B-C system is analyzed at 250 GPa which is the region of stability in the $P\bar{4}m2$ structure and the interesting pressure for T_c calculation (Fig. 2a). The observable compositions of $B_{13}C_2$, B_4C, BC_3, BC_5 and BC_7 are compared the formation enthalpy, which can determine the global minimum of structural stabilities in that pressure. The formation enthalpy (H_f) can be calculated as follows[26]:

$$H_f = \frac{H_{B_xC_y} - (XH_B + YH_C)}{X + Y}, \tag{2}$$

where H_i represents the enthalpy of the i*th* compounds in solid form, X and Y are positive numbers. By using the equation (2), the BC_7 composition presents the minimum of formation enthalpy in the B-C system at 250 GPa.

According to Fig. 2a, we also compute the phonon of the diamond-like $P4m2$ structure at 250 GPa, which presents dynamically stable as well (Fig. 2b). All lattice vibration modes are positive. Γ-point is center of the Brillouin zone (BZ). The boundaries of BZ are given by planes related to points on the reciprocal lattice. The Z point is center of a face of the BZ, while the A point is edge of the BZ. Therefore, the path of ZA mainly represents the transverse acoustic (TA) and longitudinal acoustic (LA) phonons from the lattice vibration. The TA phonons (14–28 THz) are lower frequencies than the LA phonons (30–53 THz). These phonons correspond to shear sound waves for TA, and compressional sound waves for LA. In the diamond-like and zincblende structures[27,28], it was suggested that the flattening of the TA phonon dispersion near the BZ edge can be explained with introducing long-range interatomic interactions, while the feature of TA and LA phonons in the ZA path exhibits nature of covalent bonds in this crystal. This effect is related to the oscillatory behavior in the phonon dispersion curves

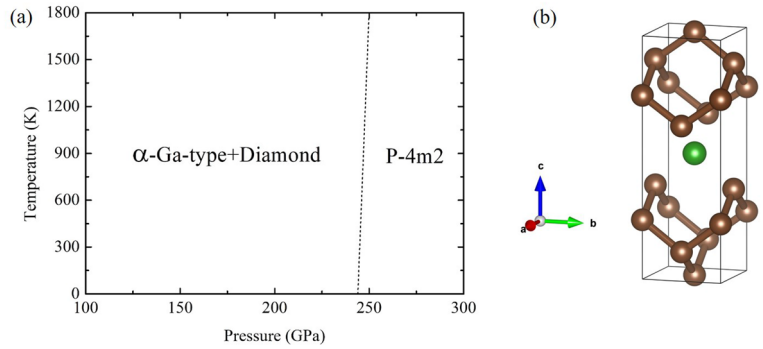

Figure 3. (**a**) Phase diagram of BC_7 and (**b**) crystal structure of the diamond-like $P\bar{4}m2$.

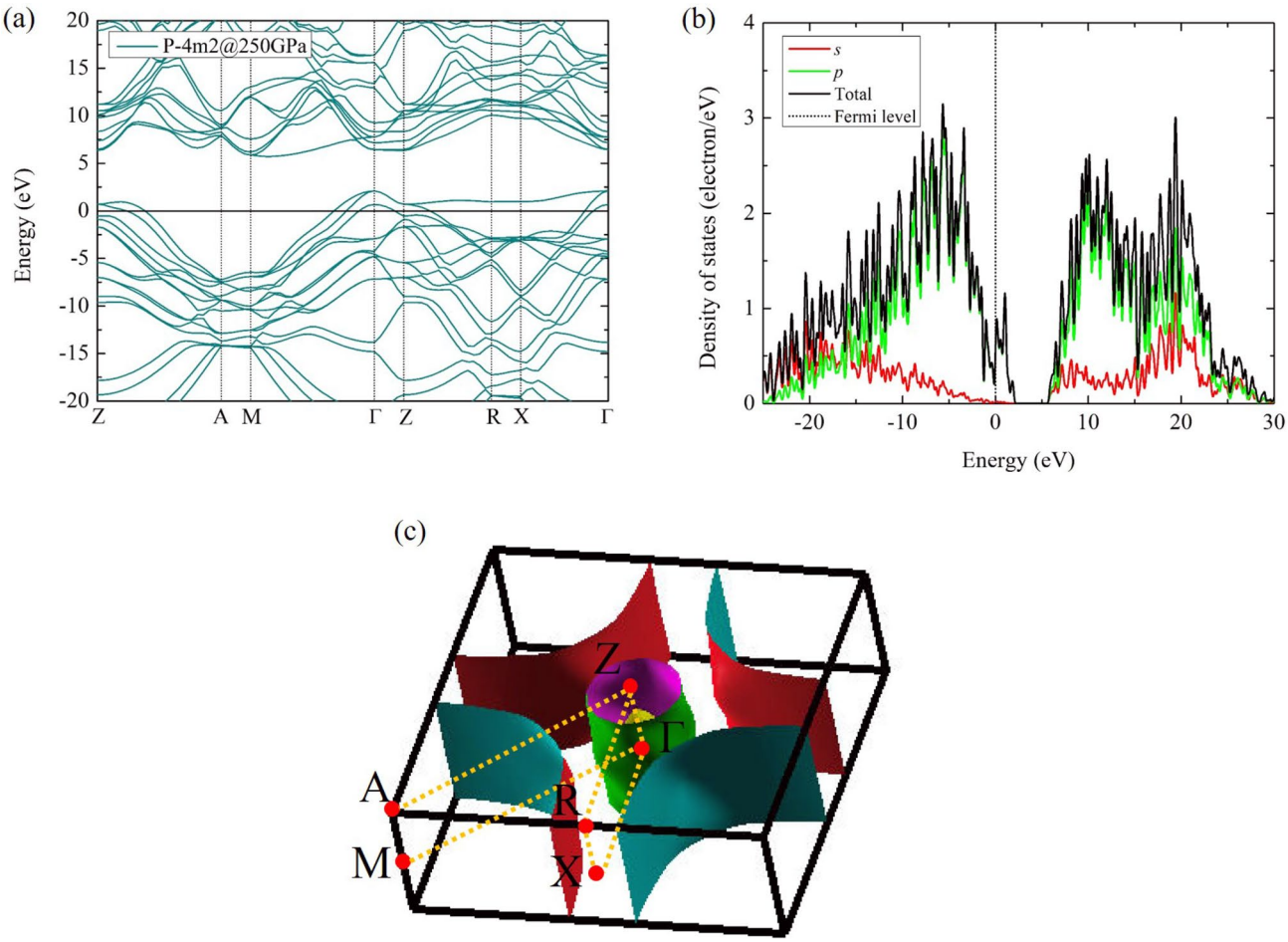

Figure 4. (**a**) Electronic band structure and (**b**) density of states of the diamond-like $P\bar{4}m2$ structure at 250 GPa and (**c**) Fermi surface of the diamond-like $P\bar{4}m2$ structure at 250 GPa.

in cubic-3C silicon carbide system which gave high energy values of vibrational energies and chemical bonds, when compared with other systems[28].

In addition, we construct a pressure–temperature (P–T) phase diagram to explore the diamond-like $P\bar{4}m2$ structure in BC_7 under temperature effect. The diamond-like $P\bar{4}m2$ is stable within the increasing of pressure and temperature monotonically (Fig. 3a). Figure 3b shows the crystal structure of the diamond-like $P\bar{4}m2$ structure.

The electronic band structure indicated the most significant result in this present study that the diamond-like $P\bar{4}m2$ structure is the metallic structure, in Fig. 4a. The remarkable solution displayed the flat band along the $Z \rightarrow R \rightarrow X \rightarrow \Gamma$-point near Fermi level. Likewise, SH_3, YH_{10}, and LaH_{10}, these flat band exhibited high-T_c superconductivity[29–32]. One of characteristic features to determine the high-T_c compounds was consulted that it depends on the Van Hove singularities (VHS) around the Fermi level in the density of states[6]. The VHS around

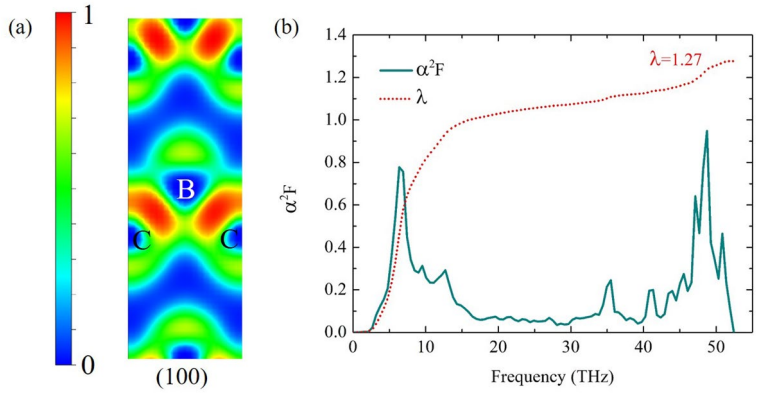

Figure 5. (**a**) The electron localization function (ELF) in the (100) atomic plane of the diamond-like $P\bar{4}m2$ structure and (**b**) the spectral function α^2F (solid line) and the integrated λ (dashed line) as a function of frequency of the diamond-like $P\bar{4}m2$ structure at 250 GPa.

		Elastic constants									
BC_7	P(GPa)	C_{11}	C_{12}	C_{13}	C_{16}	C_{33}	C_{44}	C_{66}	B	G	H_v
$P\bar{4}m2$	250	2079	473	871	0	1839	900	388	1157	649	46

Table 1. The calculated elastic constants (C_{ij}) of the diamond-like $P\bar{4}m2$ structure of BC_7 by Voigt–Reuss–Hill (VRH) method (in GPa). The calculated bulk modulus (B), shear modulus (G), and Vicker's hardness (H_v).

the Fermi level was introduced for characteristic feature of the high-Tc superconductivity in the H_3S compound[6]. They presented that the T_c of H_3S is much higher than that of H_2S, which the VHS is absent in H_2S system.

In Fig. 4c, Fermi surface (FS) shows an occupied electron on a surface in reciprocal space, which was derived from the electronic band structure. We found that the FS displayed the large sheet along the $Z \rightarrow R \rightarrow X \rightarrow \Gamma$ -point (Fig. 4c), and corresponds to the band structure and density of state (Fig. 4a,b). From the electronic band structure and the FS viewpoint, it is worth noting that BC_7 is possible to discover a high-T_c as well.

We also compute a characteristic of bonding in the diamond-like $P\bar{4}m2$ structure using the electron localization function (ELF) method[33]. The ELF displayed the tendency of an accumulated electron[34–36], with respect to a uniform electron gas of the same density. The (100) plane presents the contour plot of ELF and bonding at 250 GPa, which is a strong bonding due to an electron localization between first NN B–C is 1.449 Å(Fig. 5a). The remarkable results demonstrated metallic bond[9] under the compression as well. At this point, it is worth nothing that the strong bonding may exhibit the high-T_c.

The chemical bonding and the existence of resonance structure of BC_7 can be described by the resonating valence-bond model[37]. The delocalization of states at valence band maximum relates to the multicenter bonding of the B-C bonds in BC_7. The B atoms in diamond-like structure are bonded to their neighbors through the hybridization of electronic states. The C-rich in the BC_7 system has a hole on the B sites, due to having the lower valence electrons of B. The superposition of the orbitals from B and C is expected to induce the electron–phonon coupling constant. The coupling electronic states could induce a resonating valence-bond superconducting state. The coupled frequencies of B and C atoms in BC_5 obtained from accumulation of electrons between B and C atoms[9], relating to the systems of strong covalent bonding in H_3Se and H_3O[38].

We also calculate bulk modulus (B) and shear modulus (G), which can be obtained from elastic constants (C_{ij}) by Voigt–Reuss–Hill (VRH) method[39,40], as shown in the Table 1. The calculated C_{ij} values show all positive, and satisfy with the Born stability criteria[41], indicating the mechanical stability in the diamond-like $P\bar{4}m2$ structure at 250 GPa. The remarkable result of the C_{ij} conforms the structural stability by phonon dispersion result. By calculated from the VRH method, it is obtained that B is 1157 GPa, and G is 649 GPa. In addition, Tian et al.[42] suggested that the positive value of Vickers hardness (H_v) for an interesting material can be evaluated from B and G as follows:

$$H_v = 0.92\left(\frac{G}{B}\right)^{1.137} G^{0.708}, \tag{3}$$

By using this equation, the H_v of BC_7 at 250 GPa is 46 GPa. The solution of H_v indicates that the diamond-like $P\bar{4}m2$ presents the condition of super-hard material, which is related to the strong bonding between B and C.

The spectral function $\alpha^2F(\omega)$ of the diamond-like $P\bar{4}m2$ structure is shown in Fig. 5b, the $\alpha^2F(\omega)$ referred the electron–phonon coupling (EPC) between an initial state k_F and all other states on k_F. The calculated $\alpha^2F(\omega)$ of B and C atoms contributed to the EPC. We investigated T_c of the diamond-like $P\bar{4}m2$ structure using the Allen-Dynes modified McMillan equation[24]. We found that λ is 1.27, ω_{log} is 1498 K, using $\mu^* = 0.10$–0.13, and

Metal Carbides	Pressure (GPa)	λ	ω_{log} (K)	T_c (K)
[a] XeC_2	200	0.38	622	38
[b] BC_5	0	0.89	810	47
[c] NaC_6	0	2.92		127 (116)
[c] AlC_6	0			~ 100
[d] ClC_6	0			~ 40
[d] NaC_6	25–75			> 100
[d] AlC_6	25–175			> 100
[e] BC_7	250	1.27	1498	164 (154)

Table 2. The calculated parameters and T_c of BC_7, with solving the Allen–Dynes equations with μ^*= 0.10 (0.13). [a]Refereence[36]. [b]Refereence[9]. [c]Refereence[43]. [d]Refereence[44]. [e]This work.

T_c is 164–154 K at 250 GPa. The remarkable solutions manifested that the the diamond-like $P\bar{4}m2$ structure is the high-T_c. Likewise, binary carbon compounds with sodalite structure showed that NaC_6 is the high-T_c among of them[43]. Addition, we explored the T_c with the increased C atom, as seen in Table 2. We found that C-rich can enhance T_c at high pressure; however, we suggested that the high-T_c for carbon-rich materials may depend on the characteristic of bonding. Our results showed that carbon-rich materials is one of important effect for making the high-T_c from the strong bonding between B and C-atom (Supplementary Information S1).

Our calculation results showed that the phonon stability of BC_7 can be observed ~250GPa. In practical experiment, it is possibly to be found superconductivity of BC_7 at the lower pressure in the experiment, which was found in the shift-down of transition pressure in another material. This was discussed in the LaH_{10} system[45] that the quantum effects are important for the structural stabilities of solids with high electron–phonon coupling constants. The system could be destabilized by the large electron–phonon interaction, thus the reducing of critical pressure may be found in the synthesis.

Conclusion

In this work, we investigate the decomposition of B–C, and employed the evolutionary algorithm for finding the stable structure at high pressures. The BC_7 in the diamond-like $P\bar{4}m2$ structure exhibits as the minimum of formation enthalpy in the convex hull, and it displays structural stability at pressure above 244 GPa, and under temperature effect. The strong bonding is observed from the electron localization function. The delocalization of states at valence band maximum corresponds to the multicenter bonding of the B–C bonds, which achieves the high temperature superconductivity in BC_7. In addition, the electronics properties, such as the band structure, density of states, and the Fermi surface, are discussed as the important key to reach the high-T_c superconductivity for C-rich system at high pressure.

Received: 3 May 2020; Accepted: 28 September 2020
Published online: 22 October 2020

References

1. Zinin, P. V. *et al.* Pressure- and temperature-induced phase transition in the b-c system. *J. Appl. Phys.* **100**, 013516 (2006).
2. Zinin, P. V. *et al.* Phase transition in bcx system under high-pressure and high-temperature: Synthesis of cubic dense bc3 nanostructured phase. *J. Appl. Phys.* **111**, 114905 (2012).
3. Flores-Livas, J. A. *et al.* A perspective on conventional high-temperature superconductors at high pressure: Methods and materials. *Phys. Rep.* **856**, 1–78 (2020).
4. Drozdov, A. P., Eremets, M. I., Troyan, I. A., Ksenofontov, V. & Shylin, S. I. Conventional superconductivity at 203 Kelvin at high pressures in the sulfur hydride system. *Nature* **525**, 73–76 (2015).
5. Drozdov, A. P. *et al.* Superconductivity at 250 K in lanthanum hydride under high pressures. *Nature* **569**, 528–531 (2019).
6. Sano, W., Koretsune, T., Tadano, T., Akashi, R. & Arita, R. Effect of van hove singularities on high-T_c superconductivity in h_3S. *Phys. Rev. B* **93**, 094525 (2016).
7. Ramirez, A. P. Superconductivity in alkali-doped c60. Superconducting materials: Conventional, unconventional and undetermined. *Phys. C Superconduct. Appl.* **514**, 166–172 (2015).
8. Solozhenko, V. L., Kurakevych, O. O., Andrault, D., Le Godec, Y. & Mezouar, M. Ultimate metastable solubility of boron in diamond: Synthesis of superhard diamondlike bc_5. *Phys. Rev. Lett.* **102**, 015506 (2009).
9. Yao, Y., Tse, J. S. & Klug, D. D. Crystal and electronic structure of superhard bc $_5$: First-principles structural optimizations. *Phys. Rev. B* **80**, 094106 (2009).
10. Liu, H., Li, Q., Zhu, L. & Ma, Y. Superhard polymorphs of diamond-like bc7. *Solid State Commun.* **151**, 716–719 (2011).
11. Jay, A., Hardouin Duparc, O., Sjakste, J. & Vast, N. Theoretical phase diagram of boron carbide from ambient to high pressure and temperature. *J. Appl. Phys.* **125**, 185902 (2019).
12. Oganov, A. R. & Glass, C. W. Crystal structure prediction using ab initio evolutionary techniques: Principles and applications. *J. Chem. Phys.* **124**, 244704 (2006).
13. Kresse, G. & Furthmüller, J. Efficient iterative schemes for ab initio total-energy calculations using a plane-wave basis set. *Phys. Rev. B* **54**, 11169–11186 (1996).
14. Perdew, J. P., Burke, K. & Ernzerhof, M. Generalized gradient approximation made simple. *Phys. Rev. Lett.* **77**, 3865–3868 (1996).
15. Blöchl, P. E. Projector augmented-wave method. *Phys. Rev. B* **50**, 17953–17979 (1994).
16. Monkhorst, H. J. & Pack, J. D. Special points for brillouin-zone integrations. *Phys. Rev. B* **13**, 5188–5192 (1976).

17. Togo, A. & Tanaka, I. First principles phonon calculations in materials science. *Scr. Mater.* **108**, 1–5 (2015).
18. Savrasov, S. Y. & Savrasov, D. Y. Electron-phonon interactions and related physical properties of metals from linear-response theory. *Phys. Rev. B* **54**, 16487–16501 (1996).
19. Ma, Y., Tse, J. S., Klug, D. D. & Ahuja, R. Electron–phonon coupling of α- Ga boron. *Phys. Rev. B* **70**, 214107 (2004).
20. Haque, E., Hossain, M. A. & Stampfl, C. First-principles prediction of phonon-mediated superconductivity in xbc (x = mg, ca, sr, ba). *Phys. Chem. Chem. Phys.* **21**, 8767–8773 (2019).
21. Clark, S. J. *et al.* First principles methods using CASTEP. *Z. Kristall.* **220**, 567–570 (2005).
22. Baroni, S., de Gironcoli, S., Dal Corso, A. & Giannozzi, P. Phonons and related crystal properties from density-functional perturbation theory. *Rev. Mod. Phys.* **73**, 515–562 (2001).
23. Giannozzi, P. *et al.* Quantum espresso: A modular and open-source software project for quantum simulations of materials. *J. Phys. Condens. Matter* **21**, 395502 (2009).
24. Allen, P. B. & Dynes, R. C. Transition temperature of strong-coupled superconductors reanalyzed. *Phys. Rev. B* **12**, 905–922 (1975).
25. Katzke, H., Bismayer, U. & Tolédano, P. Theory of the high-pressure structural phase transitions in Si, Ge, Sn, and Pb. *Phys. Rev. B* **73**, 134105 (2006).
26. Weerasinghe, G. L., Needs, R. J. & Pickard, C. J. Computational searches for iron carbide in the earth's inner core. *Phys. Rev. B* **84**, 174110 (2011).
27. Peter, Y. & Cardona, M. *Fundamentals of Semiconductors: Physics and Materials Properties* (Springer, Berlin, 2010).
28. Varadachari, C. & Bhowmick, R. Ab initioderivation of a dataset of real temperature thermodynamic properties: Case study with SiC. *Modell. Simul. Mater. Sci. Eng.* **17**, 075006 (2009).
29. Papaconstantopoulos, D. A., Klein, B. M., Mehl, M. J. & Pickett, W. E. Cubic h_3s around 200 gpa: An atomic hydrogen superconductor stabilized by sulfur. *Phys. Rev. B* **91**, 184511 (2015).
30. Heil, C., di Cataldo, S., Bachelet, G. B. & Boeri, L. Superconductivity in sodalite-like yttrium hydride clathrates. *Phys. Rev. B* **99**, 220502 (2019).
31. Wang, C., Yi, S. & Cho, J.-H. Pressure dependence of the superconducting transition temperature of compressed lah_{10}. *Phys. Rev. B* **100**, 060502 (2019).
32. Papaconstantopoulos, D. A., Mehl, M. J. & Chang, P.-H. High-temperature superconductivity in lah_{10}. *Phys. Rev. B* **101**, 060506 (2020).
33. Becke, A. D. & Edgecombe, K. E. A simple measure of electron localization in atomic and molecular systems. *J. Chem. Phys.* **92**, 5397–5403 (1990).
34. Tsuppayakorn-aek, P., Luo, W., Watcharatharapong, T., Ahuja, R. & Bovornratanaraks, T. Structural prediction of host-guest structure in lithium at high pressure. *Sci. Rep.* **8**, 5278 (2018).
35. Tsuppayakorn-aek, P. *et al.* The ideal commensurate value of sc and the superconducting phase under high pressure. *J. Appl. Phys.* **124**, 225901 (2018).
36. Bovornratanaraks, T., Tsuppayakorn-aek, P., Luo, W. & Ahuja, R. Ground-state structure of semiconducting and superconducting phases in xenon carbides at high pressure. *Sci. Rep.* **9**, 2459 (2019).
37. Baskaran, G. Resonating valence bond mechanism of impurity band superconductivity in diamond. *J. Supercond. Novel Magn.* **21**, 45–49 (2008).
38. Heil, C. & Boeri, L. Influence of bonding on superconductivity in high-pressure hydrides. *Phys. Rev. B* **92**, 060508 (2015).
39. Zuo, L., Humbert, M. & Esling, C. Elastic properties of polycrystals in the Voigt–Reuss–Hill approximation. *J. Appl. Crystallogr.* **25**, 751–755 (1992).
40. Man, C.-S. & Huang, M. A simple explicit formula for the Voigt–Reuss–Hill average of elastic polycrystals with arbitrary crystal and texture symmetries. *J. Elast.* **105**, 29–48 (2011).
41. Matthew, J. . A. . D. Dynamical theory of crystal lattices by M. Born and K. Huang. *Acta Crystallogr. Sect. A* **26**, 702 (1970).
42. Tian, Y., Xu, B. & Zhao, Z. Microscopic theory of hardness and design of novel superhard crystals. *Int. J. Refract Metal Hard Mater.* **33**, 93–106 (2012).
43. Lu, S. *et al.* Superconductivity in dense carbon-based materials. *Phys. Rev. B* **93**, 104509 (2016).
44. Sano, K., Masuda, Y. & Ito, H. Superconductivity of carbon compounds with sodalite structure (2020).
45. Errea, I. *et al.* Quantum crystal structure in the 250-Kelvin superconducting lanthanum hydride. *Nature* **578**, 66–69 (2020).

Acknowledgements

We gratefully acknowledge NSC (National Computer Center, Linköping, Sweden) in Sweden for providing computing time and this research is supported by Ratchadapisek Somphot Fund for Postdoctoral Fellowship, Chulalongkorn University. This work has been partially supported by Sci Super-IV research grant, Faculty of Science, Chulalongkorn University. This research is funded by Chulalongkorn University; Grant for Research. R.A. and W.L. thank the Swedish Research Council and Swedish Research Links for financial support. P.P acknowledges all supports from Huachiew Chalermprakiet University.

Author contributions

Author contributions: R.A., P.T. and T.B. designed the research; P.T., X.Y., P.P., W.L., R.A.,and T.B. performed the research; W.L., P.T., P.P., and T.B. analysed the data; and P.T., P.P., and T.B. wrote the paper.

Competing interests

The authors declare no competing interests.

Additional information

Supplementary information is available for this paper at https://doi.org/10.1038/s41598-020-75049-x.

Correspondence and requests for materials should be addressed to T.B.

Reprints and permissions information is available at www.nature.com/reprints.

Publisher's note Springer Nature remains neutral with regard to jurisdictional claims in published maps and institutional affiliations.